Nucleosynthesis in Stars

By David Arnett
Departments of Physics and Astronomy
University of Arizona
Tucson, Az 85721, USA

Abstract

The supernova 1987A in the Large Magellanic Cloud is the brightest since the invention of the telescope. It provides an exceptional test of well-developed theoretical ideas concerning the evolution and death of massive stars. Such objects are thought to be the primary contributors to nucleosynthesis, and therefore central to understanding the evolution of galaxies. The observation of a antineutrino burst from the event provides a confirmation of the theory of gravitational collapse of stellar cores, and of modern theories of the weak interaction.

I. *Introduction*

The evolution of stars, and the use of their composition as a tracer og galactic evolution, were central themes in the work of Bengt Strömgren. Supernova 1987A has provided striking insight into these problems, and in particular into the evolution, death and heavy element yield of a massive star – just the sort of object thought to be a major contributor to nucleosynthesis.

In addition to the work presented here, that of two other groups (Nomoto *et al.*, and Woosley *et al.*) was conducted at about the same time and with similar results. Detailed references to this and other work may be found in the review by Arnett, Bahcall, Kirshner, and Woosley (1989). This discussion will focus on the broad features of what has been learned from SN1987A.

II. *Nucleosynthesis and Structure*

The first step in investigating nucleosynthesis in a star is to determine which nuclei and which reactions are to be considered. This defines a nuclear reaction network. Because of the enormous variation in reaction time it is possible (and for economy, advisable) to ignore classes of reactions and nuclei.

In Figure 1 is shown the reaction network necessary for a correct treatment of energy generation and electron capture through oxygen burning. Because of their low thresholds, ^{31}P, ^{33}S, and ^{35}Cl actively capture electrons at the densities at which hydrostatic oxygen burning occurs, and they are produced by secondary reactions in oxygen burning. This affects the star by reducing the number of electrons available

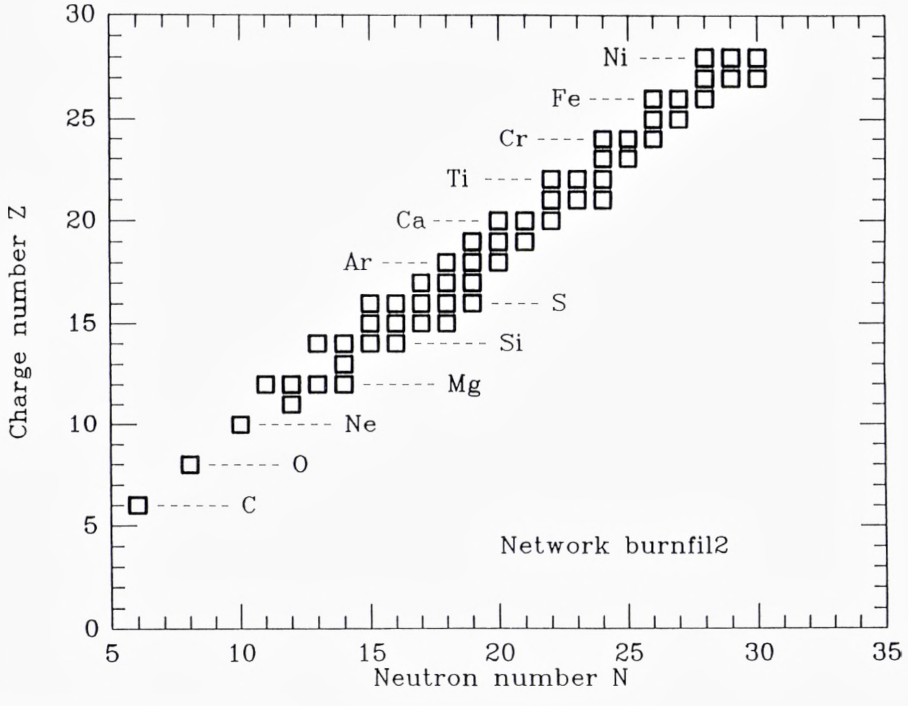

Figure 1. Reaction Network Used.

for pressure, and by reducing the energy by that carried away by $\nu\bar{\nu}$ in an URCA cycle of e-capture and decay. It affects the nucleosynthesis (and hence the energy release) by changing the ratio of neutrons to protons in the reacting matter. Consider ^{33}S: $Y_e \approx Z/A = 16/33 = 0.4848$ is in one sense optimum for the production of this nucleus. For larger Y_e there are excess protons, and for smaller values, excess neutrons. Oxygen burning proceeds, making a trace of ^{33}S. It captures an electron, reducing Y_e from an initial value of about 0.4985 toward 0.4848, which increases the amount of ^{33}S, and so on until $Y_e \approx 0.4848$. Note that the crucial quantity is neutron excess $\eta = (N - Z)/A$, which is 0.003 and 0.030 for Y_e equal 0.4985 and 0.4848, respectively; η changes by a factor of ten! Further reduction in Y_e then reduces the abundance of this nucleus, and therefore its contribution to electron capture. The process "saturates". The other two nuclei have similar Z/A, and the three dominate electron capture under typical oxygen burning conditions. The result is that Y_e approaches 0.48 and tends to stay at this value for oxygen burning. Because electron degeneracy pressure is important in supporting the stellar core, smaller core masses result. However, since the electrons are only partially degenerate, the heating/cooling implied by such processes also can modify the core mass. This entropy increase/

decrease depends upon the coupled hydrodynamics and reaction dynamics of the convective, burning flow. This problem has not been analyzed; only complete mixing approximations (spherical symmetry) have been used to date.

This matter evidently does not escape the star in large quantities. The most abundant nuclei with similar Z/A are ^{54}Fe and ^{58}Ni; they comprise only 0.1 of the solar system abundance of ^{56}Fe. This suggests that matter which undergoes *hydrostatic* oxygen burning ends as part of the neutron star; *explosive* oxygen burning occurs too fast for electron captures, and – for η near the expected value of 0.003 – tends to make an isotopic distribution like that of the solar system.

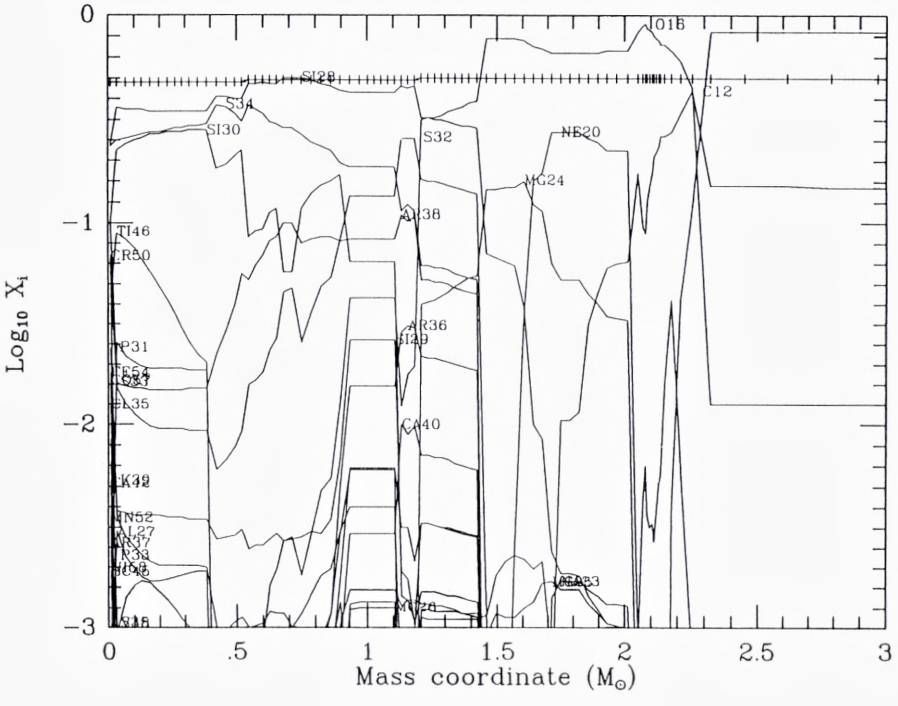

Figure 2. Detailed Abundance in the Inner 3 Solar Masses.

Figure 2 shows the complexity of the behavior of abundance versus mass coordinate in the core of an evolved massive star (Arnett 1988a). While this complication is important for understanding the approach to core collapse, the abundance patterns beyond 1.5 solar masses are considerably simpler. These are the regions that are ejected; the innermost of which have Y_e close enough to 0.5 to make the ^{56}Ni which powered the light curve of SN1987A and the daughter nucleus ^{56}Co.

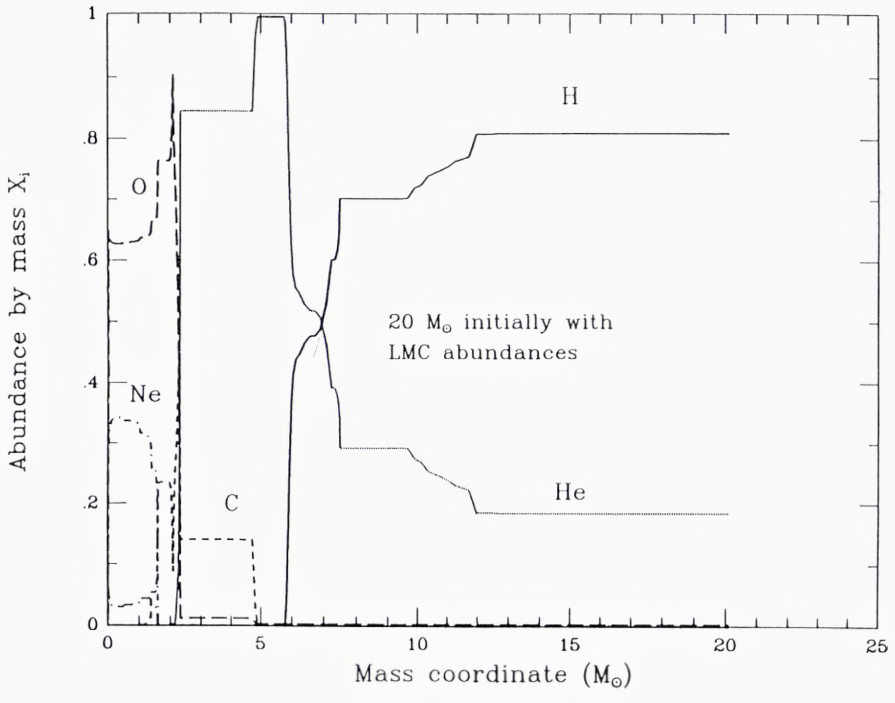

Figure 3. Abundance Structure of a 20 Solar Mass Star.

Figure 3 gives the abundance distribution of the major species for the whole star (of which Figure 2 showed the innermost region). Outside the core there is a He mantle and a H-rich envelope. There is steep density gradient between the core and the He mantle, and a lesser one between the He mantle and the H-rich envelope. The core-mantle gradient is a consequence of $\nu_e\bar{\nu}_e$ emission during carbon, neon, oxygen and silicon burning. This behavior does not occur without a direct e - ν coupling of about the strength predicted by Conserved Vector Current and Weinberg-Sahlam neutral current theory of the weak interactions, and subsequently detected experimentally. It is the pronounced core-mantle gradient which gives the small yield of ^{56}Co that was seen in SN1987A. By steep density gradient we imply a small mass which has a large range in density. At high density, Y_e is too small (*i.e.*, too neutron rich) to allow ^{56}Ni production. At low density, the shock does not heat the ejected matter enough to burn to ^{56}Ni.

A typical density structure is shown in Figure 4. The steep density gradient near 1.5 solar masses is the core-mantle interface, and is similar in stars of, say, 10 to 30 solar masses. This is the result of "core convergence" due to $\nu_e\bar{\nu}_e$ emission mentioned above. At 4 solar masses there is a smaller bump, which is the interface between the

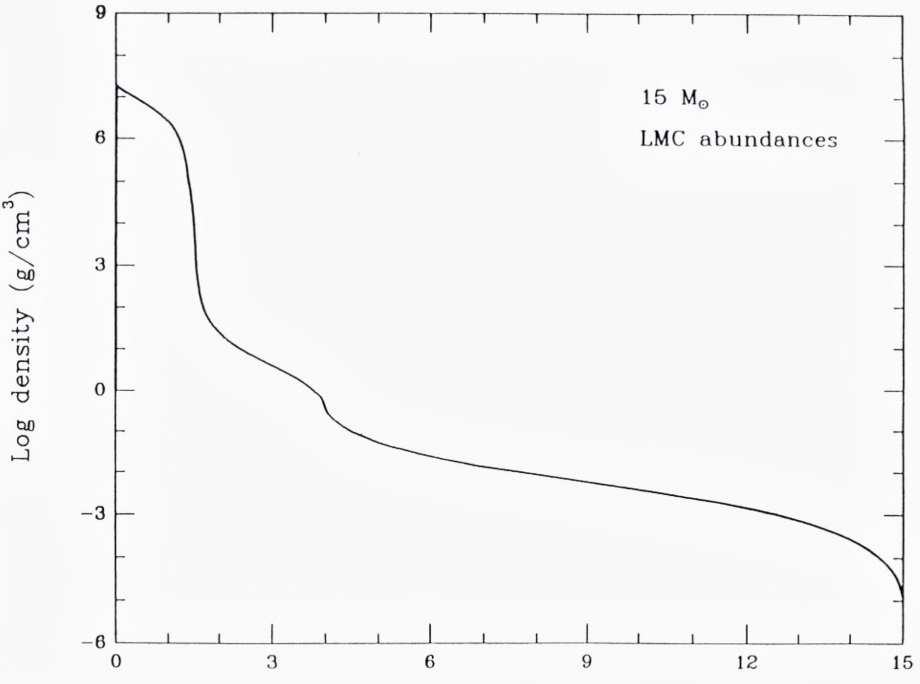

Figure 4. Typical Density Structure for a Presupernova.

He mantle and the envelope. The position in mass of this bump depends upon the mass of the star during hydrogen burning. For SN1987A we can estimate this from the luminosity of the progenitor; there is a consensus on $6 \pm 1 M_{\odot}$. This in turn suggests a initial stellar mass of 20 $M_{\odot}$ or so. The bump at the mantle-envelope interface may cause the shock to become nonspherically symmetric by generating an entropy bubble which will be Rayleigh-Taylor unstable. Asphericity was noted in the hydrogen lines at velocities appropriate to matter near this interface.

III. *The Hertzsprung Russell Diagram*

One of the major new facts that SN1987A provided was the nature of the presupernova star: it was a B3 supergiant with $M_{bol} \approx -7.8$ (the star Sanduleak -69 202; see Humphreys and McElroy 1984). Because massive stars evolve quickly and are rare, their evolution is more difficult to unravel from Hertzsprung-Russell diagrams of clusters. Young clusters are too rare and too sparse in massive stars to give good

statistical accuracy. The theoretical problem is exacerbated by the observed importance of mass loss, binary companions, and more rapid rotation. Further, the increasing importance of radiation pressure means that mixing, an irreversible process, is relatively easier in massive stars. Finally, a doubly diffusive instability involving radiation and composition called "semiconvection" is thought to be important and has certainly been controversial.

Most calculations of the evolution of massive stars through hydrogen and helium burning agreed that such objects would be red supergiants, not blue. Observed supernovae of Type II had light curves, temperatures and velocities which were consistent with the large radii of red supergiants, although it had been suggested that some massive stars might become supernovae as more compact (blue) objects (Arnett 1977).

Initial abundance seems to play a major role in producing a blue presupernova. Mass loss may be important also, but most of the hydrogen envelope must remain on the star till explosion to fit the observations (Arnett 1988a; Woosley, Pinto and Ensman 1988). Variations in the profile of the composition gradient in H has long been known to cause a massive star to make "blue loops" in the HR diagram (*e.g.*, Chiosi and Summa 1970). This could be brought about by semiconvection or other sorts of mixing of this region.

Some mass was lost prior to explosion because slow moving matter, which appears to be nitrogen rich, has been observed. Since only a few percent of H consumption is required for massive stars to covert CNO nuclei to ^{14}N, this does not necessarily imply extensive mass loss; it might imply extensive but slow mixing. Observations also seem to suggest an enhancement of He in this matter. This is consistent with such mixing, and would tend to drive the presupernova blueward (Nomoto *et al.* 1988).

Much work is necessary to sort out the complexity of this aspect of stellar evolution. Fortunately this ambiguity relates to the path to explosion more than to the nature of the object at explosion. The core and mantle structure is oblivious to the radius of the envelope (except in the extreme case that the surface convective zone reaches down into the mantle). Models which arrive by different paths to the correct region of the HR diagram, have relatively similar envelope structure as well. The problem is not whether blue presupernova models can be constructed, but *which* way nature makes them.

Figure 5 shows one way to make a blue presupernova (Arnett 1987b). The key was to use abundances one quarter of solar and Ledoux semiconvection (more or less). These models need to be modified to provide some mass loss of N-rich matter; this is easy to say, but providing the uniquely correct physical mechanism requires more effort. The presupernova had a luminosity within a factor of two of 10^5 suns; its temperature is shown by the two vertical dashed lines. For this evolution, a star of slightly below 20 $M_\odot$ would fit this error box nicely. From shock calculations of the

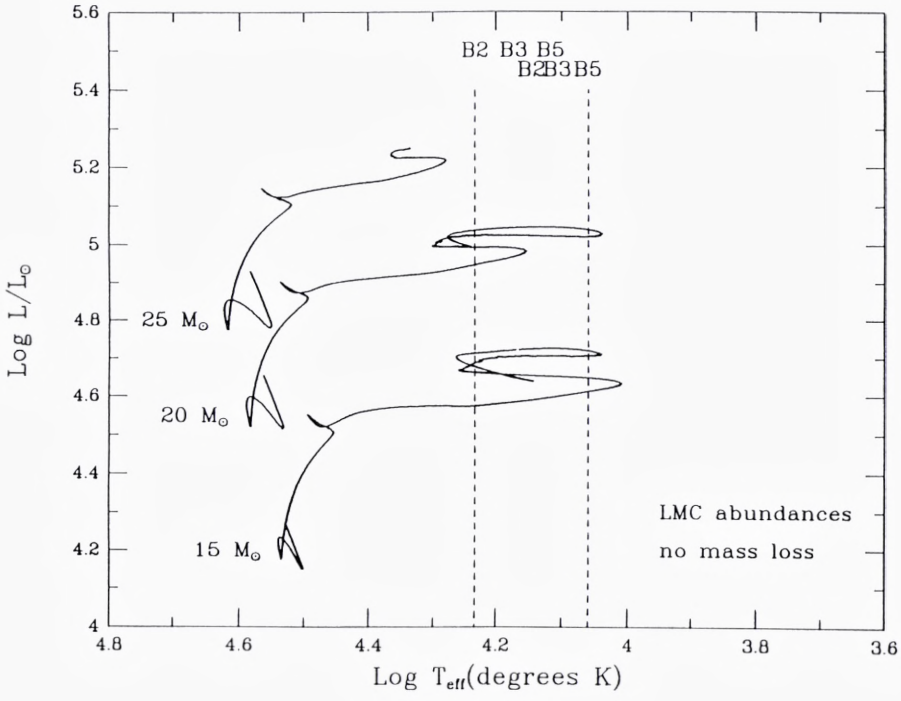

Figure 5. HR Diagram. The evolution is shown for stars of 15, 20 and 25 solar masses. The initial abundance of heavy elements ($Z > 2$) was 0.25 of solar. This is one of several ways to make a blue presupernova; it probably fails in that it does not give a trip to the red before explosion.

early light curve, to be presented below, we can infer a presupernova radius of (3 to 6) $\times$ 10^{12} cm. This passes through the error box nicely.

Theories which do not take the presupernova to have been the Sanduleak −69 202 star (*e.g.*, most binary models) clash with the first two weeks of observation of SN1987A (see below), and therefore seem unattractive.

IV. *Core Dynamics*

As the nuclear burning in the core exhausts the fuel, heat loss due to neutrino emission drives further contraction. As the compressional heating procedes (the star has an effectively negative specific heat), nuclear photodissociation occurs, giving rise to a hydrodynamic instability toward collapse. As density rises, electron fermi energies rise as well, but the threshold for electron capture on nuclei inhibits this process.

Eventually some electron capture occurs, but at sufficiently high density that the neutrinos produced do not escape freely; their diffusion time is longer than the collapse time. Thus "neutrino trapping" occurs. This inhibition of electron capture and lepton loss keeps the entropy low. Thus the inner core (a mass of about 0.7 $M_{\odot}$) collapses as a unit until it reaches nuclear density, at which point the nucleon-nucleon interaction becomes repulsive enough to stiffen the equation of state. The collapse is halted for the inner core, it rebounds, and the outer core material now rains down supersonically. A shock wave is formed which begins to propogate outward, reversing the infall and photodissociating the nuclei in the infalling matter. So far there is general agreement among theorists (see Brown 1988, and other papers in that volume).

At present the mechanism of explosion is unclear. In the "prompt shock" picture, the shock continues outward, ejecting the mantle and envelope. Unfortunately the best calculations to date agree that for realistic physics, the energy losses due to photodissociation of nuclei and to neutrino emission as the shock moves to lower densities where it becomes transparent, conspire to kill the shock. The competition is the "delayed mechanism". In this picture the shock dies (at about 20 milliseconds after bounce), but after some time (hundreds of milliseconds) heat transfer by the slowly diffusing neutrinos heats the infalling matter. As the pressure rises, the infall slows and reverses itself. This then drives off the mantle and envelope. There are no numerically reliable computation of this process as yet, just some interesting pioneering studies.

The precise nature of the explosion mechanism is important in that it determines the energy of the explosion, the mass of the condensed remnant left, and the yield of the heavy elements in the innermost region of the ejecta.

Figure 6 indicates the nature of the ejection process for a "toy" theory, in which the neutrino processes were artificially frozen to represent a limiting case in which neutrino cooling did not kill the shock (Arnett 1987c). It is to be taken as roughly representative of the sucessful realistic calculation which we still seek. The "mantle-envelope" shock (which may or may not be the "core" shock) propogates into the mantle and then the envelope, leaving behind a hot neutron star. Notice the extraordinary density gradient, comprising 18 powers of ten! The interface between the ejected mass and the edge of the new neutron star is a quasihydrostatic region, at a density near that of the post-shock matter. As the shock moves to lower densities, it lays down a hydrostatic trace which becomes the outer part of the neutron star. This trace involves increasingly less matter. This is the hydrodynamic process which determines the "mass cut". For the toy calculation shown, the explosion energy was a bit too large, the remnant mass too small, and too much deep neutron rich matter was ejected. All these problems could be solved in principle by the action of some mechanism to damp the explosion. The question is *what* mechanism? Either of the two theories mentioned above could accomplish this in principle; what did nature do?

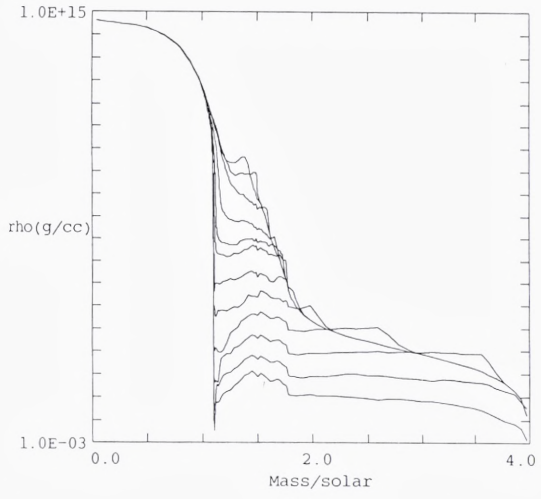

Figure 6. A Toy Model of Supernova Collapse and Explosion. By supressing neutrino transport, a hydrodynamic explosion resulted. The "mass cut" (the interface between remnant and ejecta) was carefully resolved in this calculation.

V. *Neutrinos*

The most dramatic observation of SN1987A was the detection of 11 neutrinos by the Kamiokande group (Hirata *et al.* 1987) and 8 by the IMB (Irvine, Michigan and Brookhaven) group (Bionta *et al.* 1987). There are possibly supporting observations from Baksan (Alekseev 1988). The number of facts that have been claimed to have been implied by these observations, like the number of papers concerning them, far exceed the number of events. We must not overinterpret. Statistics of small numbers are relevant here.

How many parameters may be inferred from 19 events? Every added parameter implies a division of the information content and a corresponding increase in statistical error. An astrophysicist would not be embarrassed to infer three parameters from this data, but even so the error is not negligible. For example, the three might be total energy release, neutrino temperature, and release time; these might map into the experimental data on number of neutrinos detected, energy of neutrinos detected, and time interval of detection, for example.

What was to be expected?

The energy release should reflect the binding energy of a neutron star. Typical theoretical models gave a gravitational binding energy of about 0.1 of the rest mass. Core convergence mentioned above gave core masses of roughly a Chandrasekhar mass, or about 1.5 $M_\odot$. This implies a binding energy of $B \approx 3 \times 10^{53}$ ergs.

The neutron star equation of state becomes stiff at densities at which repulsive interactions between nucleons become important. The atomic nucleus balances the attractive and repulsive nucleon forces for stability. Because these short range forces change rapidly with density, and also because the average density in a neutron star is slight less than its central value, the neutron star will settle to an average density close to nuclear density, or about 4×10^{14} grams cm^{-3}. This implies a radius of $R \approx 12$ km.

The luminosity in neutrinos of all types is the energy release divided by the diffusion time, $L \approx B/\tau$, and also the surface area times the emissivity per unit area, $L = 4\pi R^2 2 f \sigma T_e^4$, where f is the number of neutrino flavors and σ is 7/8 the usual Stefan-Boltzmann constant for photons (the 7/8 is due to Fermi-Dirac rather than Bose-Einstein statistics). This gives $T_e \approx 8.6[3/2f\tau]^{1/4}$ MeV for this radius R. For diffusion from a sphere, $\tau = 3R^2/\pi^2\lambda c$, where the mean-free-path λ is $1/N\sigma$. The number of interacting centers per unit volume is $N \approx \varrho N_A \approx 2.4 \times 10^{38}$, where N_A is Avogadro's number. The cross section is $\sigma \approx 2 \times 10^{-44} \varepsilon_\nu^2$ cm^2. Because of neutrino trapping, the lepton number is not much less than it was at the onset of collapse, $Y_e = 0.42$. The fermi momentum may then be scaled from that of the nucleon in the nucleus, which is at comparable number density. Doing this carefully gives $\mu_\nu = 100$ MeV, and $\varepsilon_\nu^2 = \mu_\nu^2/2$. Thus $\lambda = 3$ cm. In turn, this gives $\tau \approx (10^6)^2/(3(3)3 \times 10^{10}) = 3$ seconds.

Using this and assuming e, μ, and τ type neutrinos, so $f = 3$, we have $T_e \approx 5.5$ MeV. This will decrease slightly if gravitational redshift is corrected for.

Numbers of this sort were put together by many people before SN 1987A exploded, but unfortunately not concisely collected in a single publication.

From the observations (for example, see Burrows and Lattimer 1987, Bahcall, Piran, Press, and Spergel 1987, and Lamb, Melia and Laredo 1988), $B = (2 \text{ to } 4) \times 10^{53}$ ergs, $T_e \approx 3.5$ to 5 MeV, and $\tau \approx 4$ seconds. The agreement is dramatic. Unfortunately the limited number of neutrino events precludes a discrimination between the two pictures of the explosion mechanism discussed above.

VI. *Early Light Curves*

For the first two weeks the behavior of SN1987A was dominated by the effects of the shock and its heating. These were quickly calculated by dumping some amount of energy inside a presupernova model and calculating the hydrodynamics and radiative diffusion with a one dimensional hydrocode. Figure 7 shows shapshots of the structure of a representative model (Arnett 1988b). At 54 minutes the shock has reached the surface of the presupernova. Within another 50 minutes the structure has assumed a constant shape which then expands homologously. Subsequent behavior depends upon further heating and cooling.

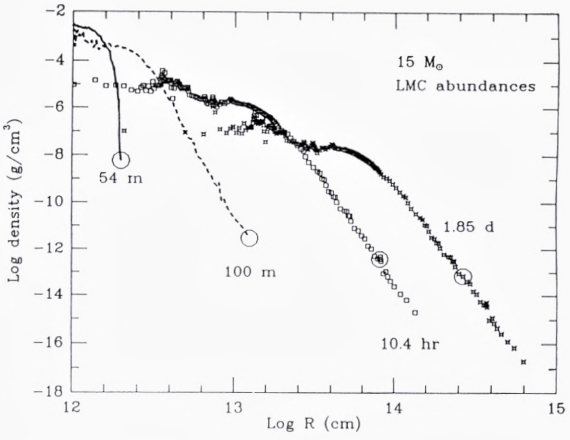

Figure 7. Snapshots of Density Structure in Supernova Ejecta.

The luminosity behaves as shown in Figure 8. The solid curve represents the visual magnitude V, and the dashed curve the bolometric magnitude. The time scale is normalized so the explosion occurred at the Kamiokande-IMB detection time for neutrinos. The theoretical curve gives a good representation of the fast rise implied by the earliest observations and limits. Note that there was a brief but intense flash, mostly in the ultraviolet, about an hour after the neutrino detection. This occurs when the shock hits the stellar surface. The agreement is good between observation and theory; the adjusted parameter is the shock energy (here 2×10^{51} ergs).

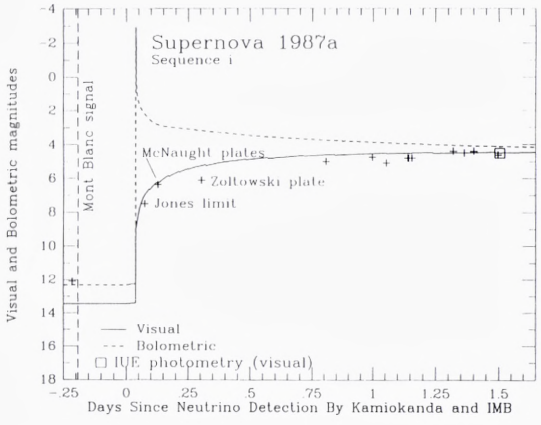

Figure 8. Comparison of Theory and Observation of the Early Light Curve of SN1987A.

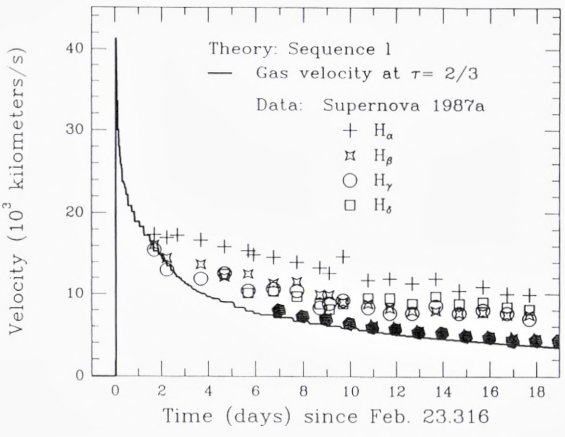

Figure 9. Velocities in SN1987A.

Figure 9 shows the change in photospheric velocity over the first few weeks. The solid curve is the theoretical model and the points are various upper limits to the photospheric velocity inferred from different spectral lines. No new parameter adjustments were made.

Figure 10 shows the change in effective temperature (now of photons, not neutrinos!) over the first few weeks. The solid curve is the theoretical model and the points are for values inferred from UBV observations (pluses) and IUE data (boxes); detalied references and discussion is to be found in Arnett (1988b). Again, no new parameters were adjusted.

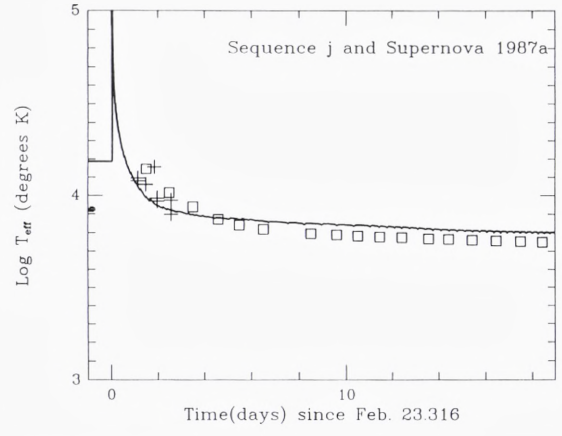

Figure 10. Effective Temperature in SN1987A.

The shock model provides a superb representation of the observational data over the first few weeks. After that, the decay of ^{56}Co becomes evident.

VII. *The Nickel Bubble*

The most tightly bound nucleus having equal numbers of protons and neutrons ($Z = N$) is ^{56}Ni. Therefore, any fuel with $Z = N$ will tend to burn to ^{56}Ni.

Hydrogen burning converts H to ^{4}He, which has $Z = N$, and rearranges the CNO isotopes to ^{14}N, which also has $Z = N$. Helium burning converts ^{4}He to ^{12}C and ^{16}O (again $Z = N$), while $^{14}N(\alpha,\gamma)^{18}F(\beta^{+}\nu_{e})^{18}O$ increases the neutron excess to $\eta = (N - Z)/A \approx 0.002$ in matter initially having solar abundance. The burning of carbon and neon change this little (to $\eta \approx 0.003$), and are essentially a rearrangement of $Z = N$ nuclei.

For $\eta \leqslant 0.003$, these fuels will burn to ^{56}Ni if heated to explosive temperatures.

With hydrostatic oxygen burning the picture changes, as discussed above, approaching $\eta \approx 0.030$. For such high neutron excess, the matter no longer burns to ^{56}Ni.

Production of ^{56}Ni indicates that matter *around* the stellar core has been *explosively* heated.

This has two implications: (1) because it is an endpoint in burning, ^{56}Ni can be made in relatively large abundance, and (2) because it is radioactive, it and its daughter ^{56}Co will store energy until they decay.

Type I supernovae have fast radiative diffusion times, so that the ^{56}Ni decay is evident, and produces the peak in the light curve. For more massive (or more slowly expanding) supernovae, a longer diffusion time will smooth out the ^{56}Ni peak, allowing the ^{56}Co one to dominate. In SN1987A this begins to occur in the third week, and is observed to continue for at least the next year and a half.

As we saw above, the ^{56}Ni is made in matter which just escapes the star, *i.e.*, just outside the "mass cut". The shock leaves the ejected matter moving almost homologously ($v \propto r$). The ^{56}Ni is therefore some of the most slowly moving matter; in models it moves at about 1,000 km/s. As ^{56}Ni decay occurs, the gamma-rays are trapped, heating the matter. This increases the pressure relative to unheated matter, setting up a pressure gradient and driving additional mass motion. A hot "nickel bubble" is formed, underlying slowly moving matter. It becomes Rayleigh-Taylor unstable, and overtakes overlying material. This intrusion gives macroscopic mixing, but the mean free paths are too small for complete microscopic mixing on this time scale.

Figure 11 shows the beginning of this process (Arnett 1988a). The horizontal scale is expansion velocity, which is proportional to radius. The top panel indicates the composition; many elements are omitted for clarity. The bottom panel shows the temperature of the matter. Two jumps are indicated. The one at higher velocity is

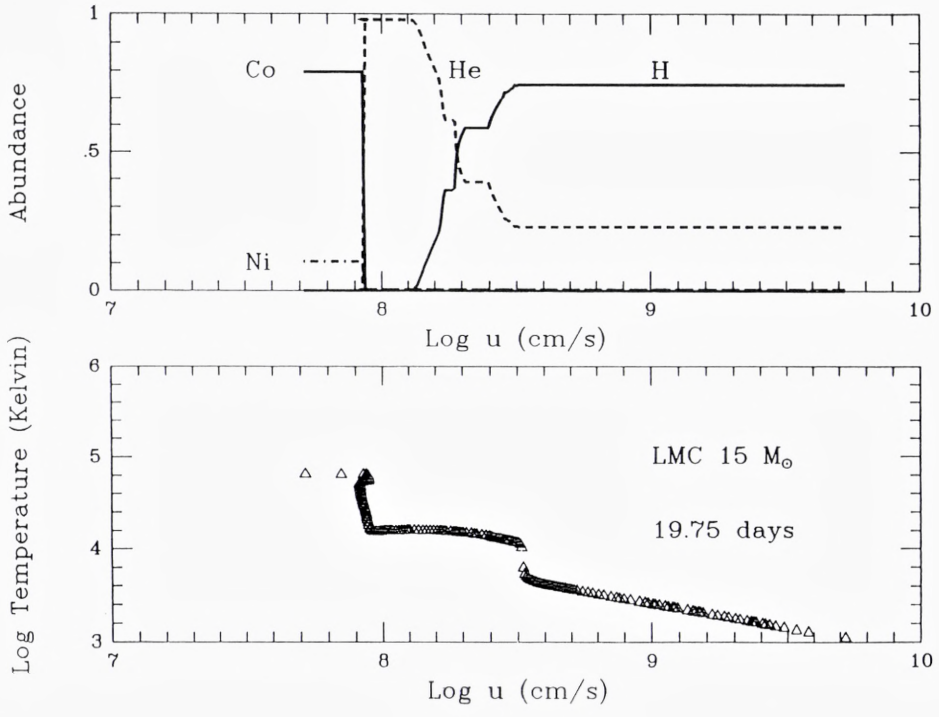

Figure 11. Temperature and Abundance of Selected Elements as a Function of Velocity at 19.75 Days after the Explosion.

due to the recession of the photosphere into the mass of the ejecta; it is a recombination wave. The one at low velocity is due to heating by ^{56}Ni decay; here the matter is Rayleigh-Taylor unstable. A multidimensional calculation is needed to follow the hydrodynamic behavior further. A crude approximation is to define a mixing velocity from the acceleration implied by the Rayleigh-Taylor instability, and microscopically mix the spherically symmetric zones. This underestimates the penetration of ^{56}Ni into overlying regions; this gives mixing up to velocities above 2,000 km/s.

Such penetration by the ^{56}Ni and ^{56}Co has dramatic implications for γ- and x-ray luminosities.

VIII. *The Light Curve at Later Times*

The expansion is homologous except for slow aspherical mixing motions at the interface between the He mantle and the H-rich envelope, and the nickel bubble. This

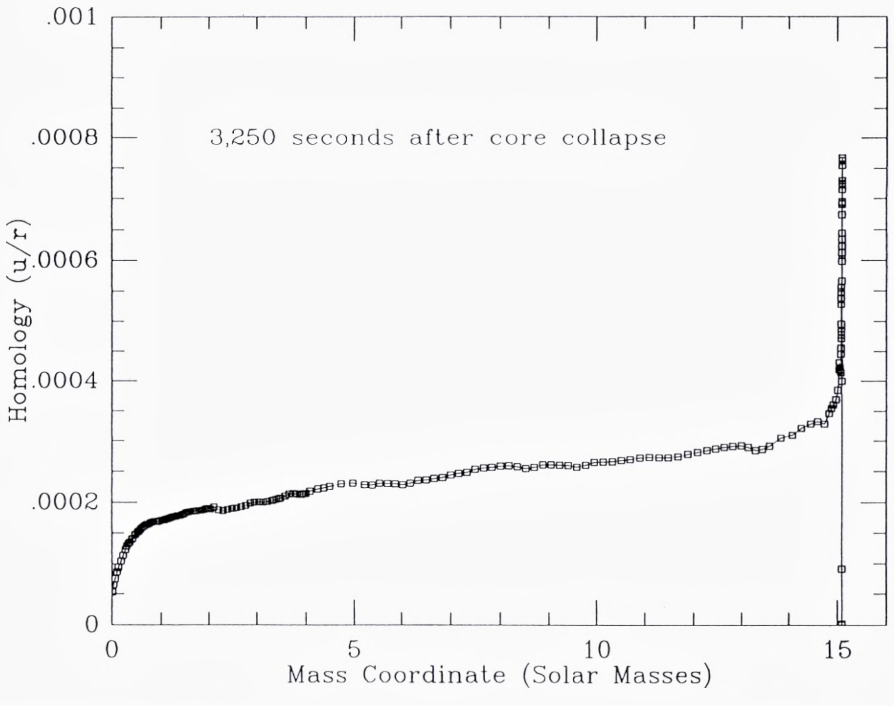

Figure 12. Homology (u/r) versus Mass Coordinate in a Supernova Model after the Shock reaches the Surface.

homology allows an accurate analytic treatment of the supernova light curve (Arnett and Fu 1989). Figure 12 explicity shows the degree of homology found in a numerical computation.

Figure 13 compares the bolometric luminosity from (1) the SAAO data (shown as crosses; Menzies *et al.* 1987, Catchpole *et al.* 1988), (2) a numerical computation (solid line), and (3) an analytic solution (open circles). The numerical solution differs from the analytic in two important ways. First, it correctly deals with the first few weeks of shock related behavior, which are not included in the analytic model (the behavior near time zero in the figure). After this poor start, the analytic solution reproduces the observations well. The numerical calculations do less well, having a jagged behavior. This is mostly due to the unrealistic assumption of strict spherical symmetry. As the recombination wave sweeps in through zones of varying composition, it is not reasonable to ignore nonspherical motions (see above) which would destroy the precise phase coherence which gives rise to the jagged effect. Numerical calculations which attempt to introduce some "mixing" do smooth out this effect.

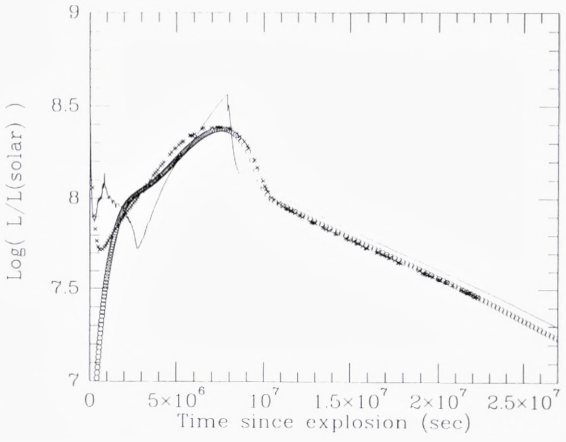

Figure 13. Comparison of Observed, Numerical and Analytic Light Curves.

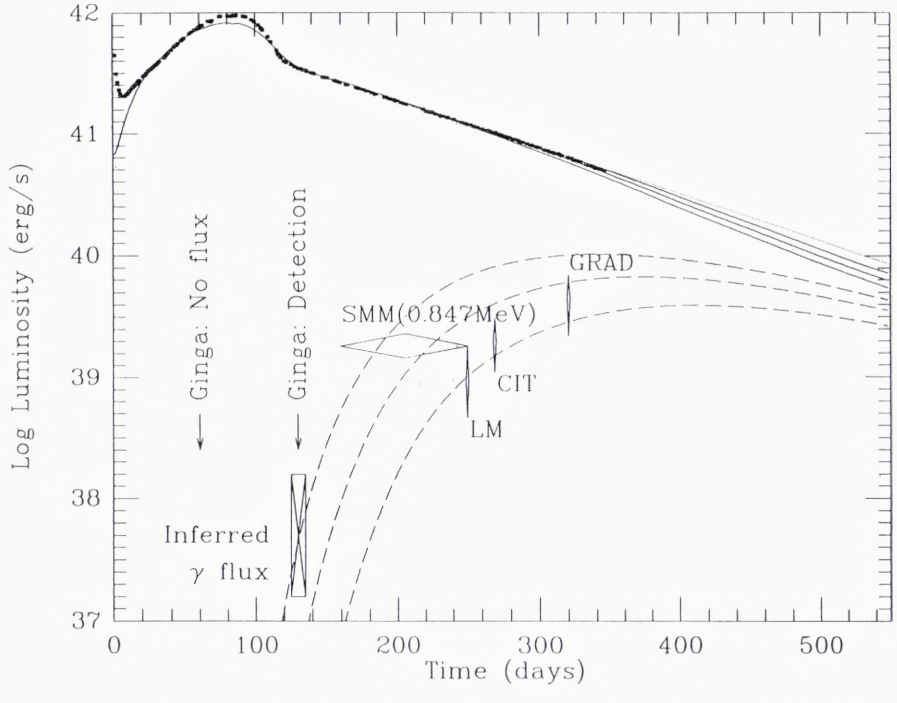

Figure 14. Thermal and Gamma Ray Light Curves for the First 550 Days of SN1987A. SAAO data are represented by solid dots, solid lines are the theoretical curves for infrared, visual and ultraviolet wavelengths combined, and dashed curves are for gamma luminosity. Several gamma line detections are shown.

Such smoothing is a natural feature of the analytic models, which use an average opacity inside the photosphere.

Figure 14 shows the light curve in "thermal" (infrared, visual, ultraviolet) radiation (solid lines) and gamma rays (dashed lines). If the first Ginga detection of *x*-rays is interpreted as due to comptonized gamma rays, the corresponding gamma luminosity can be estimated; this is shown as a crossed box. The luminosities corresponding to several detections of gamma lines are shown as diamonds, of size corresponding to quoted errors. Given the great experimental difficulty, the agreement is startling. As time passes, the easier escape of gammas will cause the "thermal" curve to sag. This has been observed. If there is another source of energy it will cause the curve to decay less steeply, or rise. The accurate exponential decay follows the meanlife of ^{56}Co quite well for the SAAO curve, but less well for the bolometric curve inferred by the CTIO group. This seems to be due to different pass bands for filters, resulting in CTIO missing some lines and therefore giving a lower limit for the luminosity (Menzies 1989). For this reason the SAAO curves are plotted; an agreement on this point by the observers would be welcome.

Figure 15 shows the light curves for still later times. Three possibilities are given,

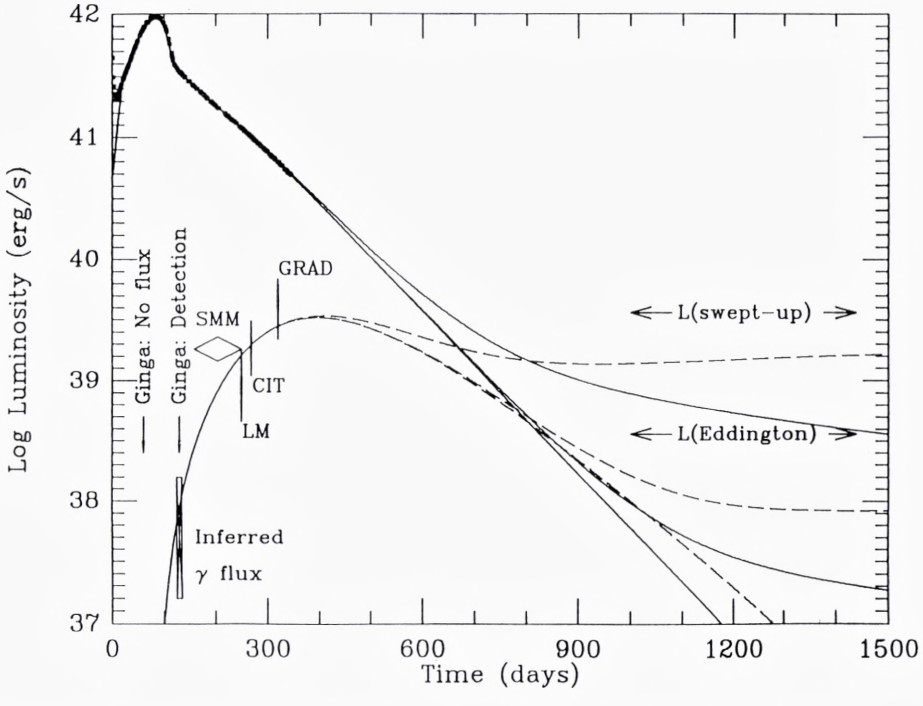

Figure 15. Similar to Figure 14, but for 1500 Days, and showing the Effects of a Possible Pulsar.

corresponding to no pulsar, a pulsar of luminosity of 10^{39} erg/s and one of 2×10^{38} erg/s. This pulsar luminosity is assumed to be emitted in e^+e^- annihilation radiation, which maximizes its chance of escape. At the time of writing, the light curve follows the ^{56}Co decay so well that no pulsar brighter than that in the Crab Nebula could be in SN1987A. It might be that the pulsar is subluminous because it rotates more slowly, or it may not yet have turned on. The neutrino detection has assurred us at least that a neutron star was formed.

Future dramatic events to be expected are the detection of the neutron star in electromagnetic radiation, and of ^{57}Co decay.

IX. *The Uniqueness of SN1987A*

Observationally, SN1987A was unprecedented. To what extent is this event anything more than a freak?

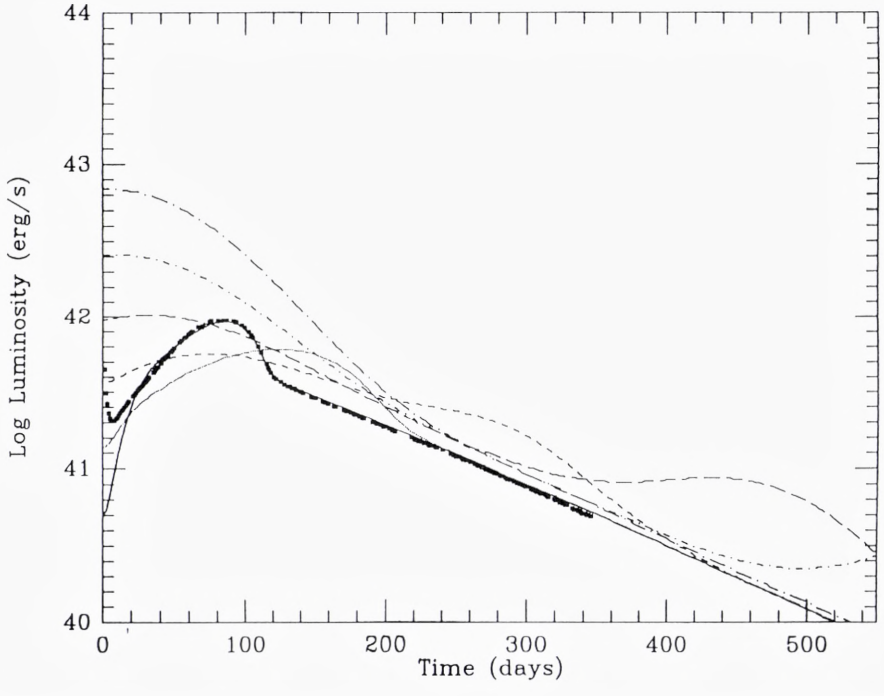

Figure 16. SN1987A and SNII. The SAAO data are shown as solid squares, and the fiducial model (Arnett and Fu 1989) which fits the data as a solid line. The sequence is of models which are identical except for radius, which increases by factors of 2.667.

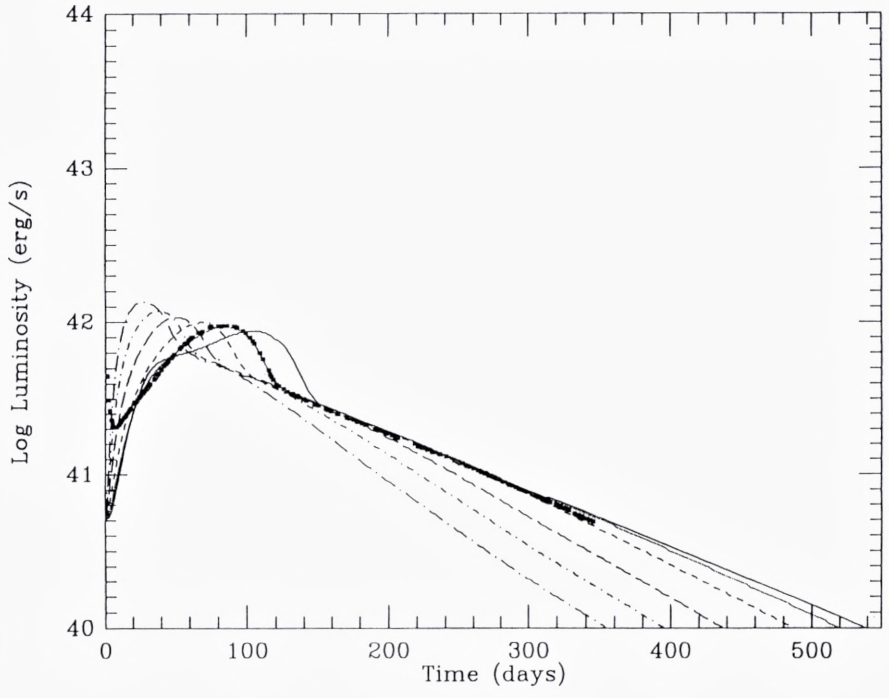

Figure 17. SN1987A and SNI. The SAAO data are shown as solid squares, and the fiducial model (Arnett and Fu 1989) which fits the data as a solid line. The total explosion energy is fixed, so that there is an increase in energy per unit mass, and therefore velocity scale, as the mass decreases.

The only thing atypical about SN1987A is probably the fact that is was exceptionally well observed. Dim supernovae are under-represented in surveys, and would not be well observed. SN1987A is likely to differ from typical Type II supernovae (that is, the ones observed till now) only in that it was a blue supergiant when it exploded, not a red one. This is a phenomenon of the envelope structure, and not of the core of mantle.

Figure 16 illustrates this point; shown are light curves for models identical to that for SN1987A except that they have increasingly larger radii. They form a sequence which extends to behavior appropriate for canonical Type II supernovae.

This is not to say there are not unanswered questions, such as the mystery spot, the disagreement with speckle and theoretical radii, the absence of a pulsar signal, the nature of the observed asphericities, and the yield of nuclei other than $A = 56$, for example. These will undoubtedly teach us more; we have already leaned much.

Further, SN1987A has a simple connection to Type I supernovae. Figure 17 shows

light curves for models identical to that for SN1987A except that they have increasingly smaller mass. This gives larger expansion velocities for the fixed explosion energy. The shorter radiative diffusion times begin to show the ^{56}Ni peak, and look like dim SNI. By increasing the mass of ^{56}Ni in these models, they would fit the light curves of Type I supernovae.

SN1987A is a natural member of a theoretical sequence, not a freak. Therefore it provides an empirical determination of the general process by which massive stars die, and of their nucleosynthesis yield. We are extraordinarily lucky to have such a splendid test of a fundamental aspect of astrophysical theory.

References

Alekseev, E. N., Alexeyeva, L. N., Krivosheina, I. V., and Volchenko, V. I. 1988, *Phys. Lett.* **B 205**, 209.

Arnett, W. D. 1977, *Ann. N. Y. Acad. Sci.*, **302**, 90.

Arnett, W. D. 1987a, *ESO Workshop Proceed.*, **26**, 373.

Arnett, W. D. 1987b, *Ap. J.* **319**, 136.

Arnett, W. D. 1987c, *Origin and Evolution of Neutron Stars*, ed. D. J. Helfand and J.-H. Huang, (Dordrecht: D. Reidel), p. 273.

Arnett, W. D. 1988a, *Supernova 1987A in the Large Magellanic Cloud*, (Cambridge: Cambridge University Press), p. 301.

Arnett, W. D. 1988b, *Ap. J.* **331**, 377.

Arnett, W. D., and Fu, A. 1989 *Ap. J.*, **340**, 396.

Arnett, W. D., Bahcall, J. N., Kirshner, R. and Woosley, S. E. 1989, *Ann. Rev. Astron. Ap.*, **27**, 629.

Bahcall, J. N., Piran, T., Press, W. H., and Spergel, D. N. *Nature* **327**, 682.

Bionta, R. M. *et al.* 1987, *Phys, Rev. Letters* **58**, 1494.

Brown, G. E. 1988, *Phys. Reports* **163**, 1.

Burrows, A. and Lattimer, J. M. 1987, *Ap. J.* **318**, L63.

Catchpole, R. M., Whitelock, P. A., Feast, M. W., Menzies, J. W., Glass, I. S., Marang, F., Liang, J. D., Spencer Jones, J. H., Roberts, G., Balona, L. A., Carter, B. S., Laney, C. D., Lloyd Evans, T., Sekiguchi, K., Hutchinson, M. G., Maddison, R., Albinson, J., Evans, A., Allen, D. A., Winkler, H., Fairall, A., Corbally, C., Davies, J. K. and Parker, Q. A. 1988, *Mon. Not. R. astr. Soc.* **229**, 15P.

Chiosi, C. and Summa, C. 1970, *Ap. Space Sci.* **8**, 478.

Hirata, K. *et al.* 1987, *Phys. Rev. Letters* **58**, 1490.

Humphreys, R. M. and McElroy, D. B. 1984, *Ap. J.* **284**, 565.

Lamb, D. Q., Melia, F., and Loredo, T. J. 1988, *Supernova 1987A in the Large Magellanic Cloud*, (Cambridge: Cambridge University Press), p. 204.

Menzies, J. W., Catchpole, R. M., van Vuuren, G., Winkler, H., Laney, C. D., Whitelock, P. A., Cousins, A. W. J., Carter, B. S., Marang, F., Lloyd Evans, T. H. H., Roberts, G., Kilkenny, D., Spencer Jones, J., Sekiguchi, K., Fairall, A. P., and Wolstencroft, R. D. 1987, *Mon. Not. R. astr. Soc.* **227**, 39P.

Menzies, J. W. 1989, preprint.

Nomoto, K., Shigeyama, T., and Hashimoto, M. 1987, *Proc. ESO Workshop on the SN1987A*, ed. I. J. Danziger, (European Southern Observatory: Munich), p. 325.

Nomoto, K., Shigeyama, T., and Hashimoto, M. 1988, *Astron. Ap.*, in press.

Woosley, S. E., Pinto, P. A., and Ensman, L. 1987, *Ap. J.*, **324,** 466.